Acta Cryst. (1979). A35, 861–870

Secondary Extinction in Rotating Single-Crystal Slabs

BY T. GIEBUŁTOWICZ, W. MINOR AND I. SOSNOWSKA

Institute of Experimental Physics, Warsaw University, ul. Hoża 69, 00-681 *Warszawa, Poland*

(*Received* 6 *January* 1978; *accepted* 5 *June* 1979)

Abstract

Variation of the diffraction conditions for neutrons in a rotating crystal frame is discussed. It is shown that the angle of deviation from the Bragg position varies with a rate equal to double the angular velocity of the crystal. This makes it possible to calculate the diffraction power for type-I Zachariasen mosaic crystals and then to obtain a solution of the Darwin equation for a rotating crystal slab with zero absorption. Further considerations refer to the space distribution of diffracted beam intensity. It is shown that, if a suitable experimental configuration is adopted, the structure factor modules can be determined from the intensity dependence on the angular velocity, and the result is independent of the mosaic-spread distribution in the sample. Results of experiments are presented.

I. Introduction

In recent years a number of papers discussing neutron diffraction by moving crystals have been published (Lowde, 1957; Brockhouse, 1961; Shull & Gingrich, 1964; Meister, 1967; Shull, Morash & Rogers, 1968; Buras, Giebułtowicz, Minor & Rajca, 1970; Buras *et al.*, 1972; Buras & Giebułtowicz, 1972; Buras & Kjems, 1973). A change in neutron wavelengths due to the Doppler effect and changes in reflection intensity have been observed. The Doppler effect may also play an important role in the process of diffraction in vibrating crystals (*e.g.* Galociova *et al.*, 1970; Buras, Giebułtowicz, Minor & Rajca, 1972; Mikula, Michalec, Chalupa, Sedláková & Petržílka, 1975). As was noticed by Brockhouse (1961), the rotation of a crystal at considerable speed may cause a decrease in extinction. This effect was discussed quantitatively by Buras, Giebułtowicz, Minor & Rajca (1970) who showed that the diffraction conditions vary as the neutron travels through the crystal, and that this is due to two effects; the 'geometrical' rotation and the Doppler effect. A formula describing the dependence $P(\omega)$ of the integrated intensity on the angular velocity of the crystal has been derived. In a more recent paper (Buras *et al.*, 1972), a method for direct determination of absolute values of the structure factors $|F_{hkl}|$ by fitting the theoretical dependence $P(\omega)$ to the experimental points was advanced. However, this method gives correct values of $|F_{hkl}|$ only if the assumed mosaic distribution function is in good agreement with the real one.

The present paper gives a more detailed discussion of the variation of diffraction conditions in rotating single-crystal frames. The solution of the Darwin equations (*e.g.* Zachariasen, 1967) for spinning single-crystal slabs is given and it is also shown that the extinction factor can be found experimentally. Analysis of the diffraction process shows that a neutron 'sees' in a rotating crystal the reflecting and transparent zones. This fact makes it possible to draw some conclusions as to the space distribution of the reflected beam intensity. It has been shown that if a suitable experimental configuration is applied, the observed intensity may be independent of the mosaic-spread distribution in the sample. Thus, $|F_{hkl}|$ as determined by fitting the theoretical relation $P(\omega)$ to the experimental points may be more accurate than when it is estimated by the method proposed earlier (Buras *et al.*, 1972).

II. The role of the Doppler effect in the diffraction process in rotating single crystals

The specimen velocity **V** 'seen' by the neutron on its path through the crystal is varying continuously, so the wave vector **k** in the moving frame changes due to the Doppler effect according to the formula

$$\mathbf{k} = \frac{m}{\hbar}(\mathbf{V}_i - \mathbf{V}), \tag{1}$$

where m is the neutron mass, $\hbar$ is Planck's constant and $\mathbf{V}_i$ is the neutron velocity in the laboratory system. The angle between **k** and the reflecting plane also varies continuously as a result of the crystal rotation. The effective variation of the deviation from the Bragg position due to these two effects can be found from simple calculations based on the modified Ewald construction for a moving lattice (Buras & Giebułtowicz, 1972). Fig. 1 shows this construction

0567-7394/79/060861-10$01.00

executed under the assumption that the incident angle φ in the spinning crystal system is close to the Bragg angle γ. The Bragg angle γ can be found by drawing an arc of radius U_i from point A to the point of intersection with the bisectrix of vector $(h/m)\boldsymbol{\tau}$. The angle of deviation from the Bragg position is defined as:

$$\varepsilon = \gamma - \varphi. \tag{2}$$

Thus

$$\sin\gamma = \sin(\varepsilon + \varphi) \simeq \sin\varphi + \varepsilon\cos\varphi, \tag{3}$$

since only small values of ε are taken into consideration. As can be seen from Fig. 1, the following formulae can be derived:

$$\sin\varphi = (V_i \sin\theta_i + V\cos\beta)/U_i, \tag{4}$$

$$\cos\varphi = (V_i \sin\theta_i + V\sin\beta)/U_i, \tag{5}$$

$$\sin\gamma = h\,\tau/2m\,U_i = V_0/U_i. \tag{6}$$

From (3) to (6) we get

$$\varepsilon = \frac{V_0 - V_i\sin\theta_i - V\cos\beta}{V_i\cos\theta_i + V\sin\beta}. \tag{7}$$

Let us consider the rotating specimen in the form of a crystal slab with the reflecting plane perpendicular to the crystal face. The axis of rotation is parallel to the crystal face and perpendicular to the experimental plane.

The xy coordinate system shown in Fig. 2 is defined as follows; the x axis is parallel to the velocity vector of the incident neutron $\mathbf{V}_i$ and the y axis is perpendicular to the reflecting plane. The angle between the x and y axes is not fixed.

Let the considered neutron be at a certain moment t at a certain point A. The radius r at point A is

$$r = x\cos\theta_i/\cos\psi = -x\cos\theta_i/\cos\beta, \tag{8}$$

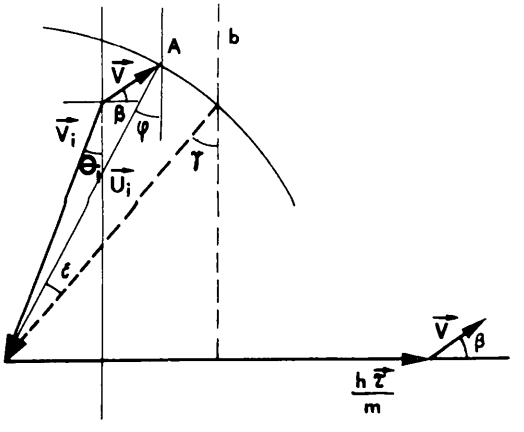

Fig. 1. Transformation of the velocity vector $\mathbf{V}_i$ from the laboratory system into the crystal system for the incident angle φ close to the Bragg angle γ. $\boldsymbol{\tau}$ is the reciprocal-lattice vector.

because $\psi = \pi - \beta$. The rotational speed being ω, the crystal velocity at point A is

$$V = |\boldsymbol{\omega}\times\boldsymbol{\tau}| = -\omega x\cos\theta_i/\cos\beta. \tag{9}$$

Hence we get the following expression for ε:

$$\varepsilon = \frac{V_0 - V_i\sin\theta_i + \omega x\cos\theta_i}{V_i\cos\theta_i + V\sin\beta}. \tag{10}$$

The variation of θ_i is described by

$$\theta_i = \theta_{i0} - \omega(t - t_0), \tag{11}$$

where t_0 is the time at which the neutron enters the crystal and θ_{i0} is the value of angle θ_i corresponding to t_0. If $V_i \gg V$ (usually $V < 10$ m/s, $V_i > 1000$ m/s), then the time dependence of coordinate x is given to a very good approximation by the equation

$$x = V_i(t - t_0) + x_0. \tag{12}$$

Then (11) becomes

$$\theta_i = \theta_{i0} - \omega(x - x_0)/V_i, \tag{13}$$

and, taking into account that for neutrons entering the crystal at various times $\theta_{i0} = \omega t_0$,

$$\varepsilon = \{V_0 - V_i\sin[\omega t_0 - \omega(x - x_0)/V_i] + \omega x\cos[\omega t_0 - \omega(x - x_0)V_i]\} \times \{V_i\cos[\omega t_0 - \omega(x - x_0)V_i] + V\sin\beta\}^{-1}. \tag{14}$$

Equation (14) describes the variation of the angle of deviation from the Bragg position with t_0 and x. $V\sin\beta$ is the only quantity in (14) which depends on x but it is small compared with the other terms in the denominator. Thus, the deviation from the Bragg angle

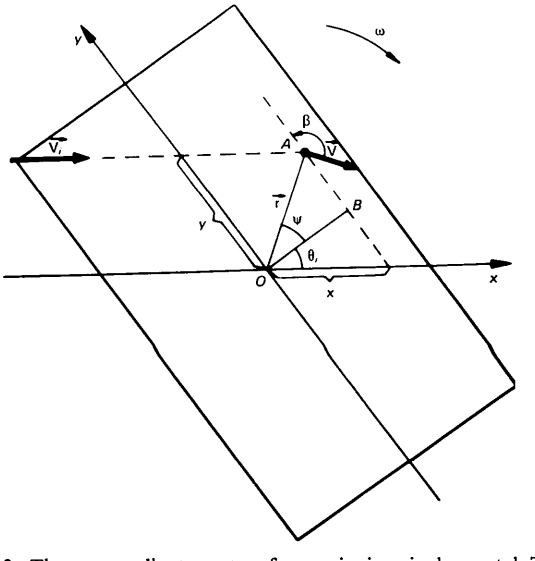

Fig. 2. The xy coordinate system for a spinning single crystal. The x axis is parallel to the velocity vector $\mathbf{V}_i$ of the incident neutron, the y axis is perpendicular to the reflecting plane, $\mathbf{V}$ is the velocity vector of the crystal at point A.

is, with a good approximation, the same for all neutrons which at a given moment are at the same depth from the crystal surface. By differentiating (14) we get ($V_i \gg V$)

$$\frac{\partial\varepsilon}{\partial x} = \frac{2\omega}{V_i}\left(1 + \frac{\varepsilon}{2}\tan\theta_i + \frac{\varepsilon\,\partial v \sin\beta/\partial x}{\omega\cos\theta_i}\right). \quad (15)$$

As stated above, these calculations refer only to angles close to the Bragg position, and thus the terms including ε are small compared with unity, and

$$\partial\varepsilon/\partial x = 2\omega/V_i. \quad (16)$$

If we take into account (12), we can write

$$\partial\varepsilon/\partial t = 2\omega, \quad (17)$$

which means that the variation in ε is twice as fast as the crystal rotation. This result can be explained as the summation of two effects; the true geometrical effect associated with the variation of angle θ_i, and the Doppler effect which varies as the neutron passes various parts of the rotating crystal. This is discussed in greater detail in the Appendix.

Considering (16) and (17), we can write

$$\varepsilon = \varepsilon_0 + 2\omega(x - x_0)/V_i, \quad (18)$$

or

$$\varepsilon = \varepsilon_0 + 2\omega(t - t_0), \quad (19)$$

where $\varepsilon_0 = \varepsilon(t_0)$ is the value of ε at the moment when the neutron enters the crystal. From (14) it can be seen that for neutrons entering the crystal at different times t_0, ε_0 is given with very good approximation by the equation

$$\varepsilon_0 = \omega t_0. \quad (20)$$

Finally,

$$\varepsilon = \omega t_0 + 2\omega(x - x_0)/V_i. \quad (21)$$

III. Extinction in a rotating single crystal

The diffraction power

In the case of neutron diffraction in a Zachariasen type-I mosaic crystal (Zachariasen, 1967), the diffraction power σ is

$$\sigma(\varepsilon) = Q\,W(\varepsilon), \quad (22)$$

where $Q = (\lambda^3|F_{hkl}|^2/\sin 2\theta)N^2$, λ is the neutron wavelength, F the structure factor, N the number of unit cells per unit volume and $W(\varepsilon)$ the distribution function of mosaic-block orientation. In this case the angle ε is defined as the deviation from the Bragg angle for the mean orientation of mosaic blocks. In a rotating single crystal, the value of ε, and hence the diffraction power, changes continuously as the neutron passes the regions of different **V**. From (21) and (22), σ is given for rotating crystal slabs by the equation

$$\sigma = Q\,W[\omega t_0 + 2\omega(x - x_0)/V_i]. \quad (23)$$

This formula describes correctly the variation of σ until a reflection occurs.

Let us assume that the neutron encounters a mosaic block in which the deviation Δ from the mean orientation is at this moment equal to ε and a reflection occurs. The value of ε at the moment of reflection is

$$\varepsilon_r = \Delta = \omega t_0 + 2\omega(x_r - x_0)/V_i, \quad (24)$$

where x_r is the x coordinate of the reflecting block. Directly after the reflection $\varepsilon = -\varepsilon_r$ (see Fig. 3), and ε varies according to the equation

$$\varepsilon' = -\varepsilon_r + \frac{\partial\varepsilon}{\partial x}(x' - x_r'), \quad (25)$$

where x_r' and x' are the coordinates of the mosaic block and the neutron, respectively, in the new coordinate system $x'y'$ in which the x' axis is parallel to the velocity vector of the scattered neutron $\mathbf{V}_r$, and y' is antiparallel to the y axis (see Fig. 3). Finally, according to (11) and (24), we obtain for the reflected neutron

$$\varepsilon' = -\varepsilon_r - \frac{2\omega}{V_r}(x' - x_r'). \quad (26)$$

Taking into consideration that $V \ll V_i$, we can assume with a good approximation that $V_r = V_i$ and $\theta_r = \theta_i = \theta$, where θ is the Bragg angle for a stationary crystal. Let z be a new coordinate axis parallel to the reflecting plane and lying in the experimental plane as shown in Fig. 4. Then,

$$z = x/\cos\theta = x'/\cos\theta, \quad (27)$$

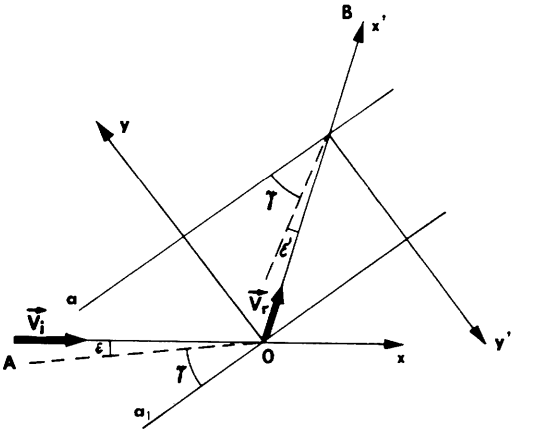

Fig. 3. Neutron reflection in a spinning single crystal: AOB is the neutron path; a, a_1 are reflecting planes; y and y' are parallel to the reciprocal-lattice vectors corresponding to reflections from both sides of the plane.

and according to (21) and (27), we get for the neutron entering the crystal

$$\varepsilon = \omega t_0 + \frac{2\omega(z - z_0)}{V_i \cos\theta}, \tag{28}$$

and for the reflected neutron according to (24), (26) and (27) we have

$$\varepsilon = -\omega t_0 - \frac{2\omega}{V_i \cos\theta}(z - z_0), \tag{29}$$

where z_0 is the z coordinate of the crystal surface. Let W be a symmetrical function. Then, according to (2), (28) and (29), (23) takes the form

$$\sigma(z, t_0) = Q\, W\left[\omega t_0 + \frac{2\omega(z - z_0)}{V_i \cos\theta}\right], \tag{30}$$

and describes the variation of the diffraction power for the incident as well as for the reflected neutrons.

Solutions of the Darwin equations

Using Zachariasen's notation (Zachariasen, 1945) the Darwin equations for stationary crystals with zero absorption generally are

$$\frac{\partial I_0}{\partial t_1} = -\sigma I_0 + \sigma I, \qquad \frac{\partial I}{\partial t_2} = -\sigma I + \sigma I_0, \tag{31}$$

where σ is constant, I_0 and I are the intensities of the incident and diffracted beams, respectively, and t_1 and t_2 are coordinates measured parallel to the incident and diffracted beams. In general, I and I_0 are functions of the positions within the crystal. For the crystal slab (symmetrical Laue case) only the z coordinate can be used and (31) reduce to

$$\frac{\partial I_0}{\partial z} = -\frac{\sigma}{\gamma} I_0 + \frac{\sigma}{\gamma} I, \qquad \frac{\partial I}{\partial z} = -\frac{\sigma}{\gamma} I + \frac{\sigma}{\gamma} I_0, \tag{32}$$

where $\gamma = \cos\theta$.

The diffraction power for the rotating slab is not constant, as it is a function of the z coordinate. The solution of (32) for such a case has been given by Buras *et al.* (1972),

$$\mathscr{P} = \tfrac{1}{2}\mathscr{P}_0(0)\{1 - \exp[(-2/\gamma)\int_{z_0}^{z_1} \sigma dz]\}. \tag{33}$$

The total power of the diffracted beam recorded in unit time can be calculated by integrating (33). Taking into consideration (30), we find that the total power of the diffracted beam is

$$P = \frac{\omega}{2\pi}\frac{\mathscr{P}_0}{2}\int_0^{2\pi/\omega}\left\{1 - \exp\left[-\frac{QV_i}{\omega}\int_0^{\xi_0} W(\omega t_0 + \xi)d\xi\right]\right\}dt_0, \tag{34}$$

where $\xi_0 = 2\omega(z_1 - z_0)/V_i \cos\theta$.

Fig. 5 shows a typical plot of the dependence of the integrated intensity $P(\omega)$ on the angular velocity ω.

For $\omega \to 0$, (34) takes the form

$$P(\omega \to 0) = \frac{I_0}{4\pi}\int_0^{2\pi}\left\{1 - \exp\left[-\frac{2z_1 Q}{\cos\theta} W(\omega t_0)\right]\right\} d(\omega t_0), \tag{35}$$

which is in agreement with the Zachariasen formula for the Laue case for a stationary crystal.

For $\omega \to \infty$ we obtain

$$P(\omega \to \infty) = I_0\, Q\, z_1 / 2\pi \cos\theta. \tag{36}$$

This result is the same as the one obtained from a kinematic approximation when the extinction effect is neglected. The $P(\omega \to 0)/P(\omega \to \infty)$ ratio gives the

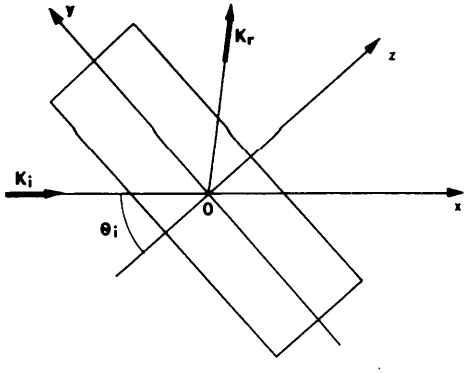

Fig. 4. Spinning crystal slab; the axis of rotation is perpendicular to the plane of the figure. The x axis is parallel to the wave vector of the incident neutron, the z axis is parallel to the reflecting plane.

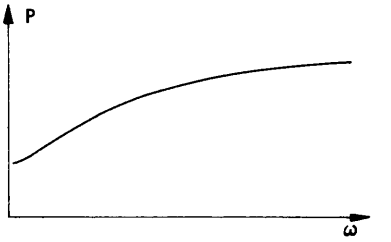

Fig. 5. Typical plot of the integrated intensity, P, *versus* angular velocity, ω.

extinction factor y defined by Zachariasen. The 'saturation' of the measured intensity $P(\omega)$ for typical values of Q and V_i is obtained for $\omega = 10^3$ to 10^5 r/min, which are available in the laboratory. This means that the extinction factor for the stationary sample can be obtained experimentally by rotating the crystal and measuring the $P(\omega \to 0)/P(\omega \to \infty)$ ratio.

Reflecting zones

When calculating the extinction corrections in stationary single crystals, the mosaic distribution function should be well defined. So far, Gaussian or Lorentzian mosaic distribution functions have usually been assumed. In the further considerations of the present paper, the only assumptions made are that the mosaic distribution function is symmetrical, $W(\Delta) = W(-\Delta)$, and that the maximum inclination of the mosaic block with respect to the mean orientation has a certain value Δ_{max}. These assumptions should be regarded as an approximation only, which optionally may be accurate. The Bragg reflection may occur when the deviation from the Bragg angle satisfies the condition $|\varepsilon| \le \Delta_{max}$. Considering (28) and (29) we get

$$|\omega t_0 + 2\omega(z - z_0)/V_i \cos\theta| \le \Delta_{max}. \qquad (37)$$

This means that a neutron entering the crystal at a given time t_0 may be reflected in a certain zone for which the z coordinate satisfies (37). This inequality is illustrated in Fig. 6(*a*). The solid lines $\varepsilon(z)$ show the dependence of ε on the z coordinate for two neutrons which enter the crystal at two different times t_{01} and t_{02}. The slope of the $\varepsilon(z)$ lines is proportional to the angular velocity ω. The reflecting zones for these neutrons, determined by the points of intersection of the $\varepsilon(z)$ lines and dashed lines $|\varepsilon| = \Delta_{max}$, are shown in Fig. 6(*b*). It should be noted that the location of the reflecting zones in the crystal depends on the entrance time t_0.

The width of the reflecting zones decreases with increasing angular velocity ω. This effect can be observed in Fig. 6(*a*) if the slope of the $\varepsilon(z)$ lines increases.

Considering (37), it is easy to show that for speeds of rotation not greater than ω_0, where

$$\omega_0 = \Delta_{max} V_0 \cos\theta / D \qquad (38)$$

(D being the thickness of the crystal), the reflecting zones are limited by the crystal surface on one side or on both sides. If $\omega > \omega_0$, the reflecting zones may be limited by the crystal surface on one side or may lie entirely inside the rotating crystal. For the sake of convenience they are hereafter referred to as boundary and internal reflecting zones, respectively.

Space distribution of reflected beam intensity

(*a*) *Analytical approach.* The fact that neutrons on their way through the rotating crystal meet transparent and reflecting zones may cause a space distribution of the diffracted beam which is not uniform.

In principle, it is possible to find this distribution by solving the Darwin equations (32), taking into account the variation of the diffraction power σ; however, even for a stationary crystal this is a difficult mathematical problem (Zachariasen, 1967; Becker & Coppens, 1974). If only the neutrons scattered by the internal reflecting zones are taken into consideration the problem becomes simpler.

Let us assume that the width of the incident neutron beam can be neglected when compared with the crystal dimensions (see Fig. 7). The width of the scattered beam measured along the ξ axis parallel to the t_1 axis (see Fig. 7), is $D/\cos\theta$. The maximum width of a boundary reflecting zone may be calculated from (37):

$$\Delta z_{max} = \Delta_{max} V_i \cos\theta/\omega. \qquad (39)$$

If $\omega > 2\omega_0$, then z_{max} is smaller than half the sample thickness $D/2$. Thus, the neutrons registered in the

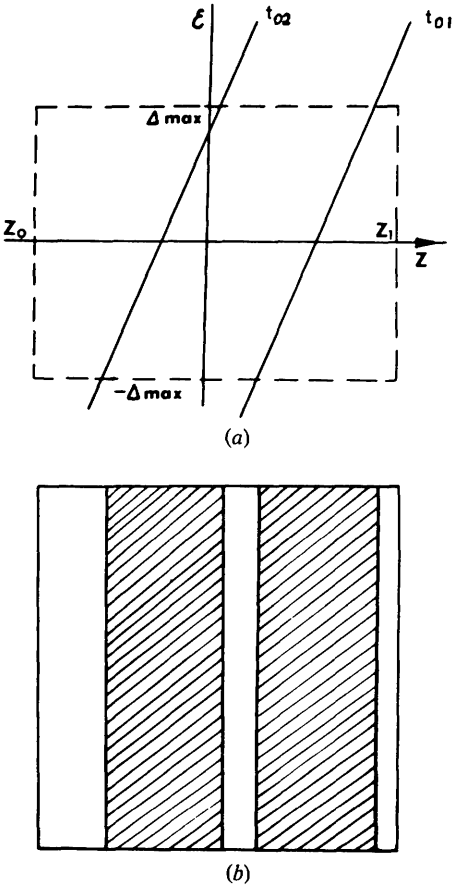

Fig. 6. Graphical illustration of inequality (37). (*a*) The dependence of ε on the z coordinate for two neutrons which enter the crystal at two different times t_{01} and t_{02}; (*b*) the corresponding reflecting zones for these neutrons.

central part of the scattered beam (ξ', ξ''), whose width is equal to

$$\xi' - \xi'' = D/\cos\theta - 2\Delta z_{max}/\cos\theta, \qquad (40)$$

were diffracted in the internal reflecting zones only.

Taking into consideration (30), Darwin equations (32), describing the diffraction in every internal reflecting zone, may always be put into the same form. Consequently, the intensity distribution function $E(\xi)$ within the interval (ξ', ξ'') should be constant.

The contribution to the total reflected beam intensity $I(t_0)\mathrm{d}t_0$ due to neutrons which enter the crystal in a time interval (t_0, $t_0 + \mathrm{d}t_0$) may be calculated from (33). Since the $W(\Delta)$ function is normalized to unity, *i.e.*

$$\int_{-\Delta_{max}}^{+\Delta_{max}} W(\Delta)\,\mathrm{d}\Delta = 1, \qquad (41)$$

one can find on the basis of (34) and (37) that for the internal reflecting zones

$$I(t_0)\,\mathrm{d}t_0 = \tfrac{1}{2}\mathscr{T}_0(0)\,[1 - \exp(-QV_i/\omega)]. \qquad (42)$$

Hence we find that the intensity distribution function is proportional to

$$E(\xi) \propto \omega[1 - \exp(-QV_i/\omega)] \qquad (43)$$

for $\xi \in (\xi', \xi'')$.

It is more complicated to find $E(\xi)$ for other values of ξ. However, it can be shown (Giebułtowicz, 1975) that the shape of the $E(\xi)$ function is characterized by two maxima on both sides of the central plateau.

(*b*) *Numerical calculations.* A computer program for more detailed calculations of the $E(\xi)$ function was used. The crystal was divided into a number of rectangles, having the coordinates j,k (see Fig. 8). The dimensions of each rectangle should be small enough to allow the change of σ within the rectangle to be neglected, thus assuming that it is constant. Assumptions were also made that the incident neutron beam was ideally collimated, monochromatic and entered the crystal at one point and that the reflection occurred every time in the center of a rectangle. The calculations were performed column by column, starting from $j = 1$ (Fig. 8). The following system of recursion equations was used:

$$\begin{aligned} I_R(j+1,k+1) &= p_j I_i(j,k) + (1-p_j) I_R(j,k), \\ I_i(j+1,k-1) &= p_j I_i(j,k) + (1-p_j) I_i(j,k), \end{aligned} \qquad (44)$$

where $I_i(j,k)$, $I_R(j,k)$ are the intensities of the beams parallel to the direction of incidence and reflection, respectively, within the j,k rectangle and p_j is the probability of reflection for column j. Since the reflection power is assumed to be constant, the formula for stationary crystals (Zachariasen, 1967) may be used;

$$p_j = \tfrac{1}{2}[1 - \exp(-2\sigma_j D/n\cos\theta)], \qquad (45)$$

where n is the number of columns and σ_j is the diffraction power for the jth column according to the equation

$$\sigma_j = QW|\omega t_0 + 2\omega D(j - 1/2)/nV_i\cos\theta|. \qquad (46)$$

It is easy to show that (44) convert to Darwin equations (32).

From the above calculations, a series of intensities $I_R(n+1, n)$, $I_R(n+1, n-2) \ldots I_R(n+1, -n+2)$ has been obtained. This series determines the intensity distribution of the reflected beam due to neutrons which enter the crystal at one given moment t_0. Thus, the procedure should be repeated for a set of different times t_0 which is analogous to integration over t_0 in the analytical approach. The results of numerical calculations are in good agreement with the conclusions of the

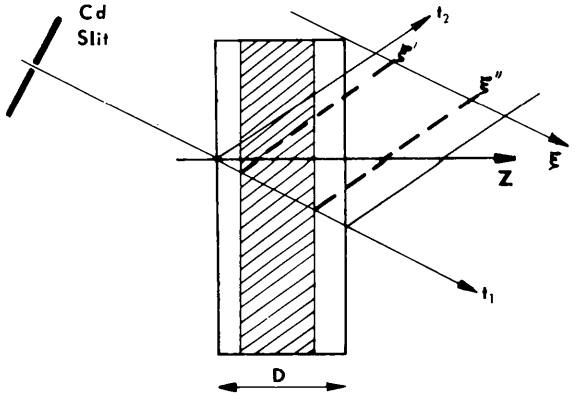

Fig. 7. Neutron diffraction in a spinning single crystal when there is a slit in the path of the incident neutron beam. The dashed area represents the reflecting area. The dashed lines illustrate the boundaries of the reflected neutron beam.

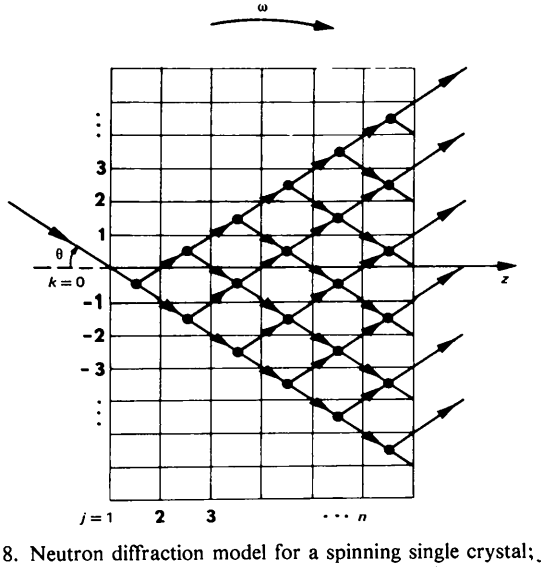

Fig. 8. Neutron diffraction model for a spinning single crystal; j,k are coordinates of the rectangular zones into which the crystal has been divided. The lines with arrows represent assumed neutron paths during the diffraction process.

analytical approach. As an example of these results, the $E(\xi)$ functions calculated for different speeds of rotation are shown in Fig. 9. The value of ω_0 for the input data used was 1000 r/min, so the central plateau did not exist at $\omega = 1500$ r/min.

IV. Experiment

The experimental measurements were performed on the TKSN-420 neutron spectrometer (Sosnowska *et al.*, 1979) at the EWA reactor in Swierk. A pyrolytic graphite monochromator was used and the collimation of the incident beam was 30′ of arc. There was no collimator between the sample and the detector. A standard BF_3 neutron counter was used and its entrance window ($\varphi = 38$mm) was located at a distance of 1·2 m from the sample. The higher-order reflections were cut off by a time-of-flight gate in the detector circuit. The rotation speed of the motor driving the crystal could be varied continuously from 600 to 12 000 r/min and it could be stabilized within this range with high accuracy, controlled by an RC generator. Bismuth single-crystal plates of thickness 8–10 mm were used as samples. The reflecting planes $(1\bar{1}0)$ were perpendicular to the crystal surface and the [111] axes were parallel to the motor axis and perpendicular to the experimental plane.

The incident beam was formed in a 1 mm cadmium slit placed between the collimator and the sample. A second slit of the same width was placed between the sample and the counter (see Fig. 10). Measurements of two types were made. In the first type the intensity distribution of the scattered beam was determined. In order to make the conditions of neutron registration constant, the scan was achieved by shifting the sample together with the motor step by step parallel to the incident beam instead of shifting the second slit. The rotation speed was constant during the whole scan of the scattered beam. In the second type the $P(\omega)$ dependence was investigated, both for the whole scattered beam without the second slit and for the central part of the scattered beam (the second slit placed in the center of the beam).

V. Results

In the preliminary measurements, the intensity distribution of the scattered beam was determined for a number of bismuth plates. The reflections $1\bar{1}0$ and $\bar{1}10$ were measured separately (for two positions of the plate). It appeared that in some cases the distributions for these two positions differ strongly, as is shown in Fig. 11. The most probable explanation of this fact is that the mosaic spread is not uniform within the whole crystal volume, as has also been observed earlier (Freund & Schneider, 1972). This supposition was

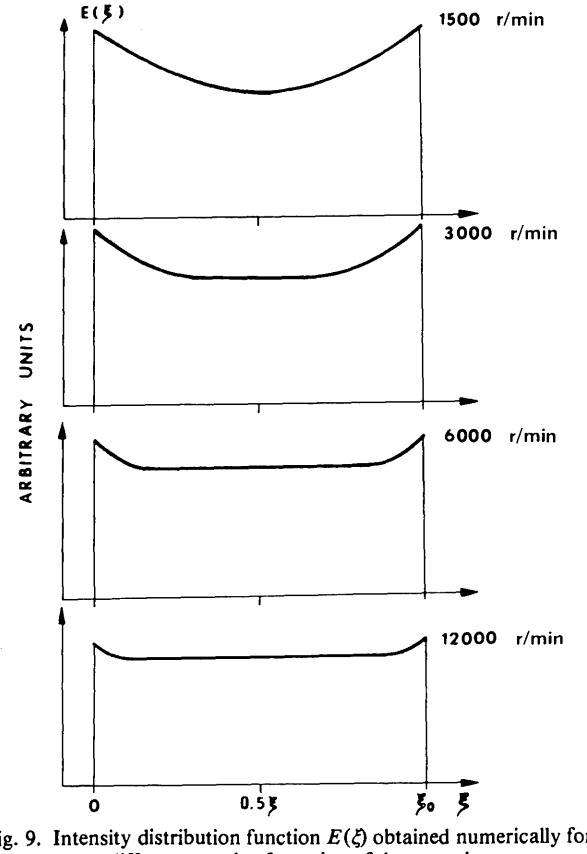

Fig. 9. Intensity distribution function $E(\xi)$ obtained numerically for different speeds of rotation of the crystal.

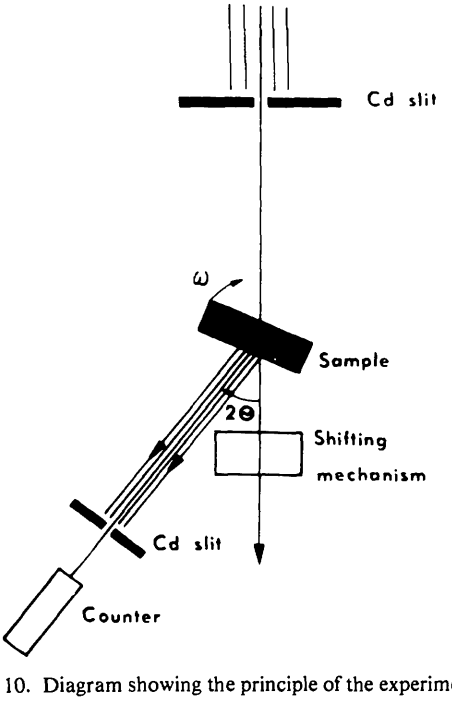

Fig. 10. Diagram showing the principle of the experiment.

confirmed by the results of calculations obtained using the computer program described above when a 'gradient' of the mosaic spread half-width was assumed. Further measurements were made for crystals in which those anomalies were not observed. The space distributions of the reflected beam were determined for various speeds of rotation and wavelengths. Fig. 12 shows the experimental results for $\omega =$ 3000 and 5400 r/min, and $\lambda = 1{\cdot}31$ and $2{\cdot}49$ Å. The results of computer calculations are presented in the same figure. The input data corresponded to the experimental conditions, and a Gaussian mosaic spread was assumed. Finite widths of the cadmium slits were also taken into account in the computer program. The measurements made for other wavelengths show similar agreement between experiment and calculations.

In the measurements of the second type, the reflection intensity was investigated as a function of the speed of rotation, both for the whole diffracted beam and for its central part. In Fig. 13, the results of these measurements are compared for one of the bismuth crystals. As is seen, the experimental relations $P(\omega)$ in these two cases are different. Curve 1 plotted in accordance with (34) is in good agreement with the experimental points $P(\omega)$ for the whole scattered beam (crosses). The variation of the intensity for the scattered beam center is described correctly by (43) for ω values greater than about 3000 r/min (curve 3). This value is in agreement with the estimated value of ω_0 [equation (42)]. Formula (43) is incorrect for $\omega < 2\omega_0$, but the theoretical relation $P(\omega)$ in this range can be found numerically using the computer calculations described above (see curve 2 in Fig. 13).

Equations (44) were tested by the least-squares fit to the experimental results obtained for different bismuth crystals. The structure factor $|F_{hkl}|$ was the fitted parameter. The results are summarized in Table 1. Some of the samples were not slabs but single-crystal cylinders with axis parallel to the axis of rotation. However, for the applied experimental geometry this difference was not significant.

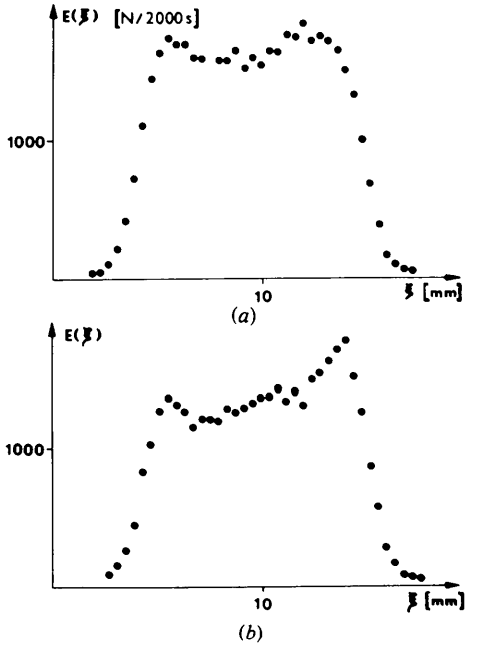

Fig. 11. Intensity distribution $E(\xi)$ obtained experimentally for reflection $1\bar{1}0$ (*a*) and $\bar{1}10$ (*b*) for the Bi crystal.

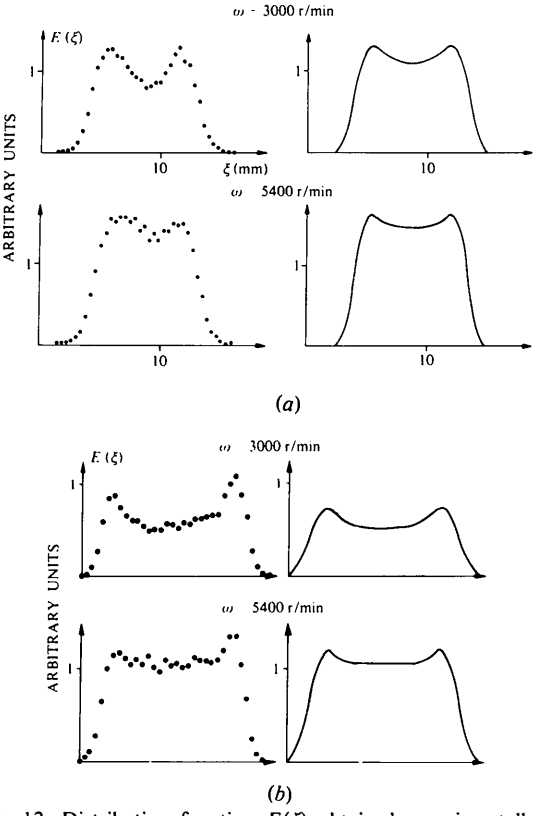

Fig. 12. Distribution function $E(\xi)$ obtained experimentally and numerically for (*a*) $\lambda = 1{\cdot}31$ Å, (*b*) $\lambda = 2{\cdot}49$ Å and $\omega = 3000$ and 5400 r/min.

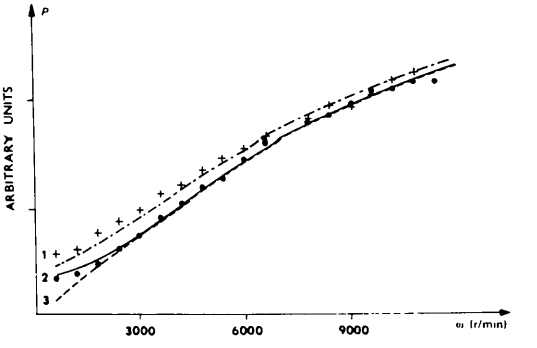

Fig. 13. Dependence of the integrated intensity on the angular velocity $P(\omega)$ for the whole scattered beam (crosses and curve 1) and bounded by cadmium slit (full circles and curve 2). Curve 3 is the plot representing formula (43).

Table 1. *Comparison of theoretical and experimental values of* $|F_{hkl}|$ *for* Bi *and* Zn *single crystals*

	D(mm)	Reflection	Extinction factor y experimental value	$\|F_E\|$ experimental value $\times 10^{-12}$	$\|F_T\|$ theoretical value $\times 10^{-12}$	Error $\frac{\|F_E\| - \|F_T\|}{\|F_T\|} \times 100\%$
I Bi	10	$1\bar{1}0$	0·064	1·61	1·62	1
		$1\bar{2}1$	0·222	1·31	1·45	10
II Bi	17	$1\bar{1}0$	0·054	1·62	1·62	1
		$1\bar{2}1$	0·189	1·32	1·45	9
III Bi	29	$1\bar{1}0$	0·125	1·52	1·62	6
IV Bi	29	$1\bar{1}0$	0·079	1·56	1·62	4
V Bi	29	$1\bar{1}0$	0·073	1·52	1·62	6
Zn	29	100	0·186	0·52	0·55	6

VI. Conclusions

It has been shown that it is possible to explain the mechanism of neutron diffraction in Zachariasen type-I rotating crystals on the basis of the theory of the Doppler effect and theory of extinction in stationary crystals. The theoretical calculations seem to be in good agreement with the experimental results concerning the increase in the diffracted beam intensity for rotating crystals and its space distribution.

As has been shown, measurement of the $P(\omega)$ function enables, when the two slits are applied, determination of the value of $|F|$ by direct fitting of the theoretical formula to the experimental points. The error in the presented results (each of them obtained for a single reflection) is no higher than 10% although it decreases with increasing extinction. Moreover, the results of fitting are not sensitive to the assumption of any type of function describing the mosaic spread distribution. Thus, the described measurement technique may present a useful tool for obtaining information from reflections with high secondary extinction. The investigation of the space distribution of the scattered beam supports the earlier observation that the mosaic structure shows considerable fluctuations in many crystals. Therefore, the assumption of the isotropic mosaic structure for a single crystal should be carefully examined. In this paper only the Zachariasen type-I crystals were considered. For the rotating type-II Zachariasen crystals, some elements of the presented model should be reconsidered, account being taken of recent papers (*e.g.* Becker & Coppens, 1974).

APPENDIX

As was said in our comment to formula (17), the angle of deviation from the Bragg position varies under the influence of two effects: the geometrical effect and the Doppler effect. It is quite natural that the contribution of the former effect to the resultant value of $d\varepsilon/dt$ is equal to the angular velocity ω of the crystal, but the reason for the contribution of the Doppler effect also being equal to ω may not be obvious. A simple explanation of this fact may be given on the basis of the Ewald construction for moving-crystal lattices (Buras & Giebułtowicz, 1972). It follows from the above paper that the fulfilment of the Bragg condition in a moving crystal depends on the projection length of the neutron velocity vector $\mathbf{U}_i$ in the moving-crystal frame on the vector $(h/m)\boldsymbol{\tau}$. The vector $\mathbf{U}_i$ varies under the action of the acceleration $\mathbf{a}'$ in the moving frame. In a rotating frame the vector $\mathbf{a}'$ is described by the known formula

$$\mathbf{a}' = -2\boldsymbol{\omega} \times \mathbf{V}_i + \boldsymbol{\omega} \times (\boldsymbol{\omega} \times \mathbf{r}), \qquad (A1)$$

where the first term is the Coriolis acceleration and the second term is the centripetal acceleration. Taking into account the values typical for an experiment (usually ω_r is not greater than 10 m/s and V_i is of the order of a thousand m/s), we can neglect the role of centripetal acceleration. Thus, the variation of ε can be considered as a consequence of the Coriolis acceleration.

The velocity of a neutron in the rotating frame is

$$\mathbf{U}_i = \mathbf{V}_i - \boldsymbol{\omega} \times \mathbf{r}. \qquad (A2)$$

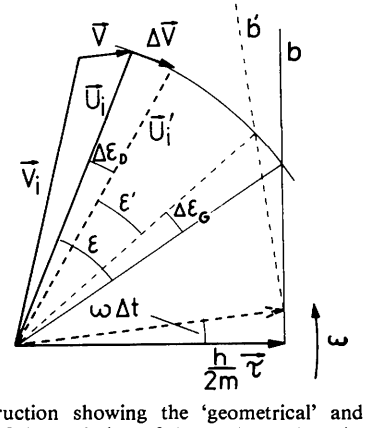

Fig. 14. Construction showing the 'geometrical' and 'Doppler' components of the variation of the angle ε. The principle of the construction is the same as for Fig. 1. The dashed lines correspond to the inclined position of the crystal due to its rotation within a small time interval Δt.

The geometrical effect is associated with the variation of $\mathbf{V}_i$ (which changes its direction only in the rotating frame), while the Doppler effect is associated with the variation of $\boldsymbol{\omega} \times \mathbf{r}$. A simple calculation in the rotating frame coordinates gives

$$d\mathbf{V}_i/dt = -\boldsymbol{\omega} \times \mathbf{V}_i \qquad (A3)$$

and, on the grounds of the approximation made above we get

$$\frac{d(-\boldsymbol{\omega} \times \mathbf{r})}{dt} = -\omega \times \mathbf{V}_i + \boldsymbol{\omega} \times (\boldsymbol{\omega} \times \mathbf{r}) \simeq - \boldsymbol{\omega} \times \mathbf{v}_i. \qquad (A4)$$

The above results show that the variations of $\mathbf{V}_i$ and $\boldsymbol{\omega} \times \mathbf{r}$ contribute equally to the Coriolis acceleration. This explains why the effects are equal.

Fig. 14 presents another simple explanation of the problem. The figure shows the 'geometrical' and the 'Doppler' components of the total variation $\Delta\varepsilon$. The value for $\Delta\varepsilon_G$ is obviously

$$\Delta\varepsilon_G = \omega\Delta t. \qquad (A5)$$

To find $\Delta\varepsilon_D$, let us consider the variation of the crystal velocity 'seen' by the neutron

$$\Delta\mathbf{V} = \boldsymbol{\omega} \times \Delta\mathbf{r} = \boldsymbol{\omega} \times \mathbf{V}_i \Delta t. \qquad (A6)$$

This means that $\Delta\mathbf{V} \perp \mathbf{V}_i$ and on the grounds of the approximations made earlier ($V \ll V_i$; $U_i \simeq V_i$), we can also assume $\Delta\mathbf{V} \perp \mathbf{U}_i$. Hence, the expression obtained for $\Delta\varepsilon_D$ is the same as for $\Delta\varepsilon_G$, *viz*

$$\Delta\varepsilon_D = \omega V_i \Delta t/U_i \simeq \omega\Delta t. \qquad (A7)$$

References

BECKER, J. P. & COPPENS, P. (1974). *Acta Cryst.* A**30**, 129–147.

BROCKHOUSE, B. N. (1961). *Inelastic Scattering of Neutrons in Solids and Liquids*, pp. 113–152. Vienna: IAEA.

BURAS, B. & GIEBUŁTOWICZ, T. (1972). *Acta Cryst.* A**28**, 151–153.

BURAS, B., GIEBUŁTOWICZ, T., MINOR, W. & RAJCA, A. (1970). *Nucl. Instrum. Methods*, **77**, 13–20.

BURAS, B., GIEBUŁTOWICZ, T., MINOR, W. & RAJCA, A. (1972). *Phys. Status Solidi A*, **9**, 423–433.

BURAS, B., GIEBUŁTOWICZ, T., MINOR, W., RAJCA, A., SOSNOWSKA, I., SLEDZIEWSKA-BŁOCKA, D. & WOJTCZAK, K. (1972). *Acta Phys. Pol. A*, **42**, 259–264.

BURAS, B. & KJEMS, J. K. (1973). *Nucl. Instrum. Methods*, **106**, 461–464.

FREUND, A. & SCHNEIDER, J. (1972). *J. Cryst. Growth*, **13/14**, 247–251.

GALOCIOVA, D., TICHY, J., ZELENKA, J., MICHALEC, R. & CHALUPA, B. (1970). *Phys. Status Solidi A*, **2**, 211–216.

GIEBUŁTOWICZ, T. (1975). *Investigations of the Influence of Crystal Motion on Extinction in Neutron Diffraction* (in Polish). Thesis, Univ. of Warsaw.

LOWDE, R. D. (1957). *Proceedings of the Meeting on the Use of Slow Neutrons to Investigate Solids and Liquids*, pp. 112–114. Stockholm: Swedish Atomic Energy Report.

MEISTER, M. (1967). *Nukleonik*, **10**, 97–101.

MIKULA, P., MICHALEC, R., CHALUPA, B., SEDLÁKOVÁ, L. & PETRŽÍLKA, V. (1975). *Acta Cryst.* A**31**, 688–693.

SHULL, C. G. & GINGRICH, N. S. (1964). *J. Appl. Phys.* **35**, 678–682.

SHULL, C. G., MORASH, K. R. & ROGERS, J. G. (1968). *Acta Cryst.* A**24**, 160–163.

SOSNOWSKA, I. *et al.* (1979). To be published.

ZACHARIASEN, W. H. (1945). *Theory of X-ray Diffraction in Crystals*. New York: John Wiley.

ZACHARIASEN, W. H. (1967). *Acta Cryst.* **23**, 558–564.